

The AdvCam project: Designing the future cameras for the Large-Sized Telescope of the Cherenkov Telescope Array Observatory

M. Heller^{a,*} on behalf of the CTAO-LST Project

*^aDépartement de Physique Nucléaire, Faculté de Sciences, Université de Genève,
Quai Ernest Ansermet 24, CH-1205 Genève, Switzerland*

E-mail: matthieu.heller@unige.ch

An international collaboration composed of Italian, Japanese, Spanish and Swiss institutes, is developing the advanced camera (AdvCam), the next-generation camera for Imaging Atmospheric Cherenkov Telescopes, designed specifically for the Large-Sized Telescopes (LST) of the Cherenkov Telescope Array Observatory. AdvCam incorporates cutting-edge Silicon Photomultipliers (SiPMs) and a fully digital readout system, setting new standards for performance and efficiency.

The upgraded camera will feature four times more pixels for the same field of view as the existing PMT-based camera, enabling finer image resolution and significantly improving angular precision and background noise rejection. To cope with the increase in number of pixels, many technological challenges are being tackled, from low power and high speed integrated chip design to real-time data processing on hardware accelerators.

This technological leap will lower the energy threshold by allowing operation at lower observation threshold and providing brighter images. The increase in effective area, angular and energy resolution will enhance the sensitivity, unlocking new potential for gamma-ray astronomy. In this work, we present the performance of the AdvCam's core building blocks and its innovative architecture capable of enabling unprecedented triggering capabilities. We also showcase the latest performance results based on Monte-Carlo data that has been tuned to reflect the latest stages of the on-going technological developments, highlighting the transformative capabilities of this next-generation instrument.

39th International Cosmic Ray Conference (ICRC 2025) in Geneva, Switzerland

*Speaker

© Copyright owned by the author(s) under the terms of the Creative Commons Attribution-NonCommercial-NoDerivatives 4.0 International License (CC BY-NC-ND 4.0). All rights for text and data mining, AI training, and similar technologies for commercial purposes, are reserved. ISSN 1824-8039. Published by SISSA Medialab.

<https://pos.sissa.it/>

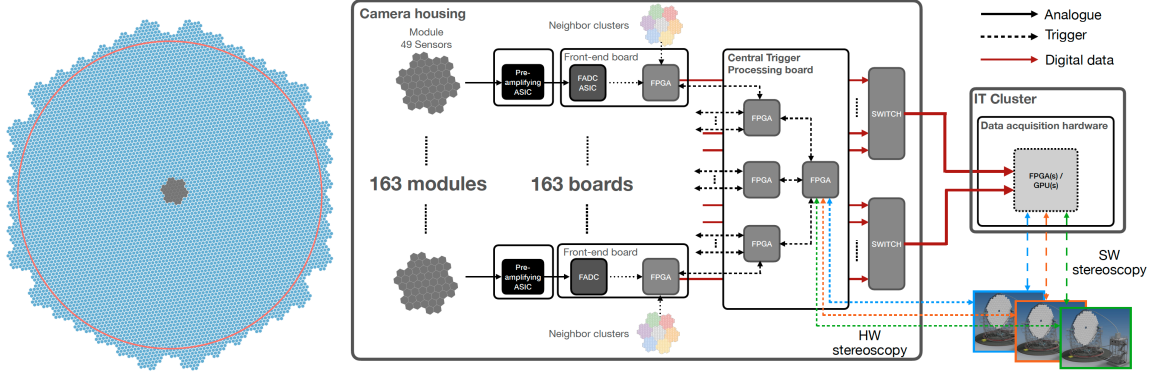


Figure 1: Left: View of the AdvCam geometry, built out of 7987 pixels. The greyed region in the center shows the size of one optical module while the red circle illustrates a field of view of 4.3° , equal to the existing camera one. Right: Simplified readout architecture, from the pre-amplification of the SiPM signals to the storage in the IT cluster of CTAO.

1. Introduction

The Advanced Camera (AdvCam) [1] is a next-generation instrument proposed for the long-term operation of the Large-Sized Telescopes (LSTs) [2] of the Cherenkov Telescope Array Observatory (CTAO), which is expected to operate for ~ 30 years. This exceeds the typical lifespan of current photomultiplier tube (PMT)-based cameras, making a robust, low-maintenance, and high-performance alternative increasingly attractive. AdvCam is designed to offer improved sensitivity, extended sensor durability and intelligent data processing to suppress background more efficiently close to the detector level.

The system builds on the expertise gained from the current LST and SST-1M SiPM camera developments [3], integrating fully digitizing electronics, reprogrammable trigger logic, and AI-based trigger and data handling. In this work we present the camera design, the current status of its implementation and its performance derived on Monte Carlo simulations.

2. The AdvCam design

2.1 The overall architecture

The proposed camera, which geometry is shown in Figure 1–left, will be composed of 163 modules of 49 hexagonal pixels each for a total of 7987 pixels and a minimum field of view of 4.3° . Each pixel features a hollow light guide with an opening of linear size ~ 2.4 cm corresponding to $\sim 0.05^\circ$. A hexagonal SiPM of latest generation is located at the output. The pixels are arranged in group of seven, a central one and six neighbours, called flower. Seven flowers are put together to form a super-flower of 49 pixels. As shown in Figure 1–right, the SiPM output is amplified by an application specific integrated circuit (ASIC) whose main design drivers are the speed and the power consumption. The analogue output of the ASIC is fed to a fast analogue to digital converter (FADC) whose digital output is streamed to powerful field programmable gate array (FPGA), common to the 49 pixels of a module, located on the front-end board (FEB). Each FEB also connects to the FEBs of the six neighbouring modules in order to build the L1 trigger which is

described in 2.2.4. When a positive L1 trigger decision is registered by a module, a signal is sent to the Central Trigger Processor Board (CTPB) which can perform a more advanced trigger decision based on the information collected by all FEBs.

As detailed in [4], spatio-temporal clustering as well as real-time inference using artificial intelligence algorithms can be deployed on the CTPB for further data volume reduction. The CTPB also connects to all other surrounding large-sized telescopes to build a hardware stereo trigger.

If the event is validated, the CTPB will issue a trigger signal to all front-end boards, prompting them to transmit data via the Remote Direct Memory Access (RDMA) over Converged Ethernet (RoCE) protocol to compatible network and data processing hardware located in the observatory building where the data acquisition and on-site data analysis will run. This protocol was chosen to enable the use of commercially available off-the-shelf components.

2.2 Photo detection plane

The development of the photo detection plane is performed jointly by the UniGe together Nagoya University and the Institute of Cosmic Ray Research. The photo detection plane will be composed of hexagonal SiPMs, identical in size to those used in [4]. The baseline technology for the sensor is the S13360-3050/75CN-UVE, which is a evolution of the S13360 technology with enhanced sensitivity to UV and faster response time. As shown in [5], to achieve very short single photoelectron response, the first prototype sensor features a large quenching resistor which affects the stability of the SiPM response under varying Night-Sky Background (NSB) conditions. This resistor will be decreased in the final sensor version to maintain the pulse full width half maximum while decreasing by four the recharge time. Since the first development, Hamamatsu has also developed a process to apply optical coating onto the SiPM surface to cut-out photons with wavelengths >540 nm thus rejecting the first peak of the background light spectrum. Alternatively, as shown in [5], the coating of the light-guides can be adapted to perform this task although with a lower efficiency as a non-negligible fraction of the light reach the sensor surface without being reflected on the light-guide surface.

2.2.1 The pre-amplifying ASIC

The front-end electronics of the telescope camera play a critical role in ensuring the accurate and efficient readout of signals from the silicon photomultipliers (SiPMs). The main design challenges consist in preserving a fast response and single photoelectron resolution while managing the high capacitance associated with large-area sensors and minimizing the power consumption. In order to verify the compliance with the application requirements, a prototype ASIC was developed at University of Geneva (UniGe) using a standard CMOS 65 nm technology node. The ASIC offers several key features: AC coupling with the camera pixels to avoid baseline shifts caused by NSB; active summation for optimal signal reconstruction with improved signal-to-noise ratio; support for multiple digitization schemes via dedicated pseudo-differential and single-ended processing channels; and compatibility with various SiPM types through tunable capacitors and amplifier current settings.

The ASIC has been tested together with the S13360-3075CS-UVE SiPM from Hamamatsu. Using a high-gain configuration for the ASIC provides an optimal noise performance which allows

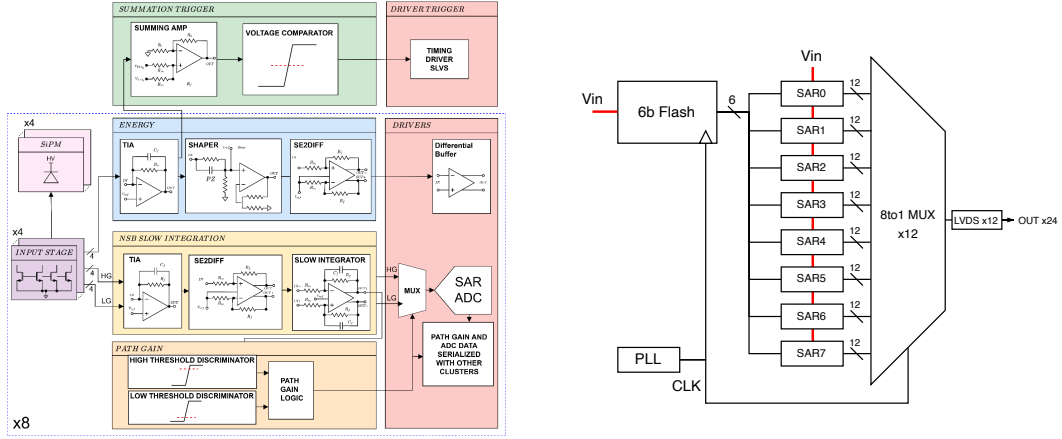


Figure 2: Left: Architecture of the PRESSEC ASIC being developed for the AdvCam. Right: Block diagram of the FADC ASIC

to distinguish individual peaks up to ~ 30 photo-electrons (p.e.). The signal-to-noise ratio¹ (SNR) reaches its maximum at 1 p.e., of 6.98 ± 0.22 . The ASIC's dynamic range, with high gain, extends up to 800 p.e. with a power consumption of 23 mW per pixel. Moreover, within the expected operational range of 1–250 p.e., FANSIC provides a full width at half maximum (FWHM) of 3 ns and a post-calibration linearity within 5%. The full characterization results are detailed in [6]. A second iteration of the ASIC has been designed and will be submitted during the summer of 2025, featuring eight single ended and differential outputs with improved pulse shape.

The final ASIC, the PRESSEC (Preamplifier Readout Electronics for Summing SiPMs Enhanced Circuit) developed in collaboration with University of Barcelona and Polytechnic University of Catalonia, will have a different architecture with enhanced performance and functionalities as shown in Figure 2. The energy path, which will provide continuous amplified waveform will have the same characteristics as the FANSIC ASIC in term of SNR, dynamic range and speed. The linearity should be kept below 3% without calibration. A slow integrator with adaptable gain will allow monitoring of the night sky background level useful for implementing feedback loop for the trigger and SiPM signal conditioning. The analogue to digital converted for this path will be added to the ASIC. Not shown in this scheme, it will be possible to inject a calibration pulse to test the sanity of the readout chain. Eventually, and even though not necessary as the trigger will be digital, an analogue trigger path will be also available.

2.2.2 The FADC ASIC

Two fast ADC ASIC prototypes for the AdvCam have been developed by the group of EPFL/AQUA². Both designs aim to achieve >800 MS/s sampling, 12-bit resolution, and <200 mW power. The first version of the ASIC, fabricated in 110 nm, combined Flash and time-interleaved successive approximation register (TI-SAR) stages but failed to meet specifications due to architectural and process limitations, yielding only 3-bit output. The second version of the ASIC,

¹defined as $SNR(N_{pe}) = G(N_{pe}) / \sqrt{\sigma_e^2 + N_{pe} \sigma_s^2}$, where $G(N_{pe})$ is the electronics gain at a given number of p.e. N_{pe} , σ_e and σ_s being the electronics and sensor noise.

²École Polytechnique Fédérale de Lausanne, Advanced Quantum Architecture Laboratory

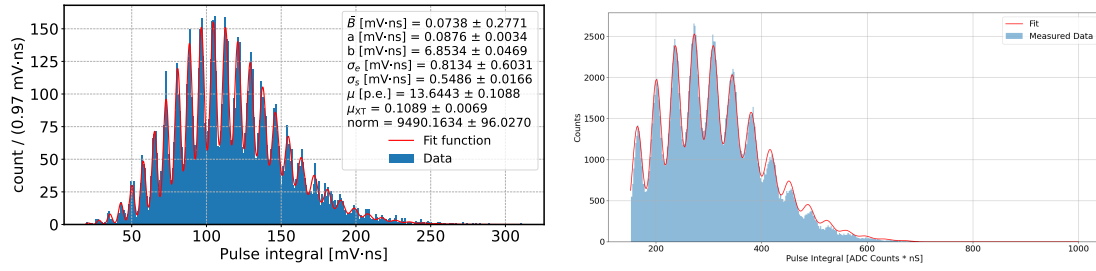


Figure 3: Left: Multi Photo-Electron (MPE) spectrum obtained with the FANSIC connected to a 5 GSps oscilloscope with 16 bits resolution, giving a single p.e. SNR of 6.5. Right: MPE obtained with the FADC board prototype with 1 GSps with 9 bits resolution, giving a single p.e. SNR of 4.5.

implemented in 65 nm CMOS, uses a 6-bit Flash front-end followed by 8x6-bit TI-SAR ADCs and achieves 1 GS/s with 12-bit resolution (see Figure 2). Key system components—phase locked loop, low voltage differential signaling and serial peripheral interface—are operational, and measurement campaigns are ongoing. Early results from the 6-bit Flash indicate correct high-speed functionality (800 MHz), with TI-SAR testing in progress. The full chain, including FPGA readout and high-speed serialization, is in place for integration with preamplifiers and system-level testing.

2.2.3 The Front-End board

The AdvCam FADC board prototype developed by INFN/Padova digitizes 12 SiPM channels at 1 GS/s with 9-bit resolution. During the first stage of board development, the data was transmitted via JESD204C over Firefly optical links to the back-end board, a Kintex Ultrascale test board from Xilinx (KCU105). However, as said above, the final solution, a custom low-resource RoCEv2 RDMA core on FPGA has been deployed allowing direct data transfer to server or GPU memory. A report on the performance of this board can be found here [7]. The FADC board was successfully tested with the FANSIC chip described in Section 2.2.1, showing a 1 p.e. SNR of 4.5 compared to 6.5 obtained with an oscilloscope. The multi photo electron spectra in both cases are shown in Figure 3. The future version, called front-end board (FEB) aims to eliminate the front-end analogue chain, integrate White Rabbit synchronization³, and scale to 49 channels with full DAQ and trigger functionality on board.

2.2.4 The L1 trigger

The first trigger level, dubbed L1 trigger, runs in the FEB and is the results of the discrimination of the sum of the digital signals of any combination of 49 pixels, a so-called L1 trigger region, with the granularity of a flower. Each FEB is connected to its six direct neighbour and collect the sum data from the neighbouring flowers, ensuring that there are no trigger dead spaces. Any positive L1 trigger leads to a second event validation performed by the second level trigger performed in the CTPB. To achieve the second level trigger, a binary stream is built for each flower indicating whether the sum of its seven pixels is above a certain threshold, different from the L1 trigger threshold. The implementation of the L1 trigger as well as the binary stream for the L2 trigger is performed by CIEMAT/Spain. Up to now, the logic has been implemented on a test bench composed of an

³<https://white-rabbit.web.cern.ch>

ADCQJ1600EVM TI board connected to KCU105 Xilinx demonstration board. The firmware for the digital sum, as well of the generation of the binary stream for the flower threshold running at 1 GHz, have been implemented together with rate counters. The implementation for 49 pixels and 6 μ s of buffer depth fits well within the allocated budget, mostly constrained by the management of the FADC stream.

2.2.5 The Central Trigger Processor board

The CTPB is being designed by the University Complutense Madrid (UCM) group to implement an L2 stereoscopic trigger combining the binary streams collected from the 163 front-end boards via optical links. The architecture involves three Kintex UltraScale FPGAs for processing of the trigger stream. Each of this three FPGA received data from a third of the camera pixels. Finally, a fourth FPGA for L2 logic, timing, and stereo coordination. Currently, two test benches are being developed: one for testing gigabit transceivers for high-performance applications and FireFly integration, and another for firmware development and testing trigger algorithms.

2.2.6 The L2 trigger

The L2 trigger will start with a spatio-temporal clustering trigger specifically running prior to the stereoscopy in order to better extract the shower timing and its location in the camera FoV, allowing for more accurate coincidences: the better shower front timing extraction allows to reduce the coincidence width improving the signal to noise ratio while the shower location enable a topological trigger. The UniGe has proposed the DBScan⁴ algorithm to perform the task proving to be extremely efficient. However, porting it to FPGA is not ideal as it is not parallelisable nor has a fixed latency. The Haute École du Paysage, d'Ingénierie et d'Architecture (HEPIA) in Geneva proposes a similar approach, relying on 3D convolutions that is fully parallelisable and therefore achieves throughput of 350 MHz with latency of below 15 ns when implemented on FPGA. Alternatively, UCM is studying implementation of deep learning models for real-time inference. Based on the CTLearn [8], light models are being tested to perform discriminations between noise events and showers, as well as between gamma and hadrons. Until now, throughput of few tens of kHz have been achieved with latencies of the order of few μ s. At this moment, these performance makes it more suitable for running after stereoscopy.

More details about those algorithms and the trigger gain are given in [4].

2.3 Data Acquisition

To address the high data throughput requirements of the AdvCam, the RoCE protocol has been adopted for its low-latency, high-bandwidth capabilities and compatibility with off-the-shelf hardware, such as NVIDIA ConnectX network cards. This allows direct memory access with minimal CPU involvement, enabling real-time data transfer and processing. A prototype implementation by INFN/Padova demonstrated stable 9.7 Gb/s transfers using a custom RDMA core on a Xilinx FPGA, integrated within the SLAC Ultimate RTL Framework (SURF) firmware framework. The approach aligns with proven network-based event building strategies in particle physics, as used at the Large Hadron Collider, and offers scalability for future developments within modern high-performance

⁴Density-Based Spatial Clustering of Applications with Noise

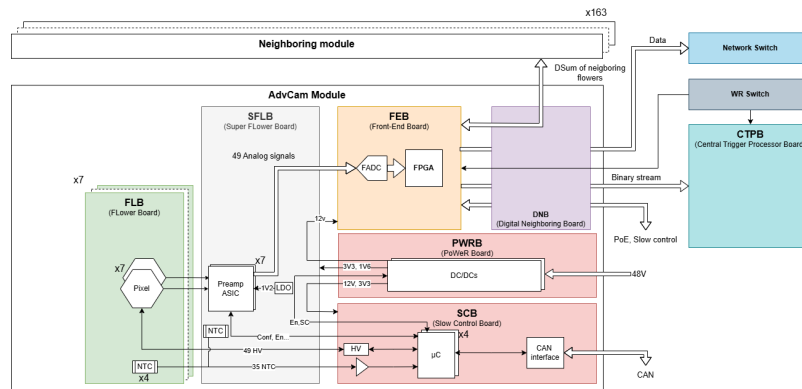


Figure 4: Architecture of the prototype module being developed for the AdvCam.

computing environments. Once the data packets are collected, the event building will be performed allowing for further real-time deep-learning inference for better gamma/hadron rejection.

3. Optical module prototype

The optical module development for AdvCam is progressing with a new architecture centered on the integration of SiPMs and with the updated FANSIC v2 ASIC on the Super Flower Board (SFLB) (see Figure 4). The effort is lead by the UniGe in collaboration with INFN/Padova and Swiss industries. The FLB schematic is under outsourced design, with interface pinouts defined for connections to both the Super Flower Board (SFLB). The SFLB has finalized its architecture and interface specifications, and will include a 4-channel DAC for voltage reference control. Concurrently, the Slow Control Board (SCB) and Power Board (PWRB) have completed architectural definition, with active component selection underway. The next steps focus on completing schematics and layouts, and finalizing inter-board interfaces for prototype fabrication. The completion of the first module prototype is foreseen for Q1 2026.

4. The AdvCam Monte Carlo performance

4.1 Stereoscopic performance using Random Forest based analysis

We compared the instrument response Functions for LSTs equipped with the current camera versus the AdvCam, using the magic-ctape framework [9], which allows for stereoscopic reconstruction. The simulation results show that The AdvCam configuration significantly enhances sensitivity below 40 GeV compared to the current PMT cameras with standard analysis cuts. It is worth mentioning that the improvement is not only related to the replacement of the PMTs by SiPMs, which increase the sensitivity to Cherenkov light, but as well by the higher image granularity.

4.2 Stereoscopic performance using deep learning analysis

To fully exploit the enhanced sensitivity of the AdvCam for faint low-energy events, a novel IACT analysis scheme has been developed within CTLearn [8]. The approach leverages advanced image cleaning using DBSCAN clustering on waveform data, generating temporally resolved masks

that preserve shower development. These masks feed into convolutional neural networks (CNNs) for gamma/hadron separation, energy, and direction reconstruction. The unprecedented challenge is to cope with the abundance of faint and nearly featureless images that are recovered. The preliminary results are promising but the training process requires additional development to fully exploit those faint events.

5. Conclusions

The architecture of the AdvCam architecture has been defined and first prototypes of various sub-systems have been built for validation. The required performance being met, the collaboration is now focusing on interfacing all the sub-systems together and scaling them to the final number of channels. A first complete optical module is expected early 2026. Recent Monte-Carlo simulations and analysis with state of the art data pipelines confirm the improved performance of the AdvCam, especially below 40 GeV. However, lowering the energy threshold, thanks to the sensor sensitivity increase and enhanced triggering capabilities poses new challenges with the need to properly account for the abundance of faint and nearly feature less events. It is worth eventually noting that the proposed design is perfectly suited for the Medium-Sized Telescopes of CTAO as well.

References

- [1] M. Heller et al. *The next generation cameras for the Large-Sized Telescopes of the Cherenkov Telescope Array Observatory*. In Proceedings of Science, volume 444, page 740, Nagoya, Japan, July 2023. URL: <https://hal.science/hal-04181692>, doi:10.22323/1.444.0740.
- [2] D. Mazin et al. *Large size telescope report*. In AIP Conference Proceedings, volume 1792. AIP Publishing, 2017.
- [3] C. Alispach et al. *The SST-1M Imaging Atmospheric Cherenkov Telescope for gamma-ray astrophysics*. Journal of Cosmology and Astroparticle Physics, 2025(02):047, February 2025. doi:10.1088/1475-7516/2025/02/047.
- [4] L. Burmistrov et al. *The trigger design for AdvCam*. these proceedings, ICRC 2025.
- [5] Kazuki Abe et al. *Characterization of SiPM and development of test bench modules for the next-generation cameras for Large-Sized Telescopes for Cherenkov Telescope Array*. PoS, ICRC2023:635, 2023. doi:10.22323/1.444.0635.
- [6] Luca Giangrande et al. *FANSIC: A fast analog SiPM interface circuit for the readout of large silicon photomultipliers*. Nuclear Instruments and Methods in Physics Research Section A: Accelerators, Spectrometers, Detectors and Associated Equipment, 1077:170523, 2025. URL: <https://www.sciencedirect.com/science/article/pii/S0168900225003249>, doi:10.1016/j.nima.2025.170523.
- [7] F. Marini et al. *FPGA-Based RoCEv2-RDMA Readout Electronics for the CTAO-LST Advanced Camera*. IEEE, July 2025.
- [8] Ari Brill, Bryan Kim, Daniel Nieto, Tjark Miener, and Qi Feng. *CTLearn: Deep learning for imaging atmospheric Cherenkov telescopes event reconstruction*, March 2018. doi:10.5281/zenodo.6842323.
- [9] H. Abe et al. *Performance of the joint LST-1 and MAGIC observations evaluated with Crab Nebula data*. Astronomy and Astrophysics, 680:A66, December 2023. arXiv:2310.01954, doi:10.1051/0004-6361/202346927.

Full Author List: CTAO-LST Project

K. Abe¹, S. Abe², A. Abhishek³, F. Acero^{4,5}, A. Aguasca-Cabot⁶, I. Agudo⁷, C. Alispach⁸, D. Ambrosino⁹, F. Ambrosino¹⁰, L. A. Antonelli¹⁰, C. Aramo⁹, A. Arbet-Engels¹¹, C. Arcaro¹², T.T.H. Arnesen¹³, K. Asano², P. Aubert¹⁴, A. Baktash¹⁵, M. Balbo⁸, A. Bamba¹⁶, A. Baquero Larriva^{17,18}, V. Barbosa Martins¹⁹, U. Barres de Almeida²⁰, J. A. Barrio¹⁷, L. Barrios Jiménez¹³, I. Batkovic¹², J. Baxter², J. Becerra González¹³, E. Bernardini¹², J. Bernete²¹, A. Berti¹¹, C. Bigongiari¹⁰, E. Bissaldi²², O. Blanch²³, G. Bonoli²⁴, P. Bordas⁶, G. Borkowski²⁵, A. Briscioli²⁶, G. Brunelli^{27,28}, J. Buces¹⁷, A. Bulgarelli²⁷, M. Bunse²⁹, I. Burelli³⁰, L. Burmistrov³¹, M. Cardillo³², S. Caroff¹⁴, A. Carosi¹⁰, R. Carraro¹⁰, M. S. Carrasco²⁶, F. Cassol²⁶, D. Cerasole³³, G. Ceribella¹¹, A. Cerviño Cortínez¹⁷, Y. Chai¹¹, K. Cheng², A. Chiavassa^{34,35}, M. Chikawa², G. Chon¹¹, L. Chytká³⁶, G. M. Ciccari^{37,38}, A. Cifuentes²¹, J. L. Contreras¹⁷, J. Cortina²¹, H. Costantini²⁶, M. Croisnionier²³, M. Dalchenko³¹, P. Da Vela²⁷, F. Dazzi¹⁰, A. De Angelis¹², M. de Bony de Lavergne³⁹, R. Del Burgo⁹, C. Delgado²¹, J. Delgado Mengual⁴⁰, M. Dellaiera¹⁴, D. della Volpe³¹, B. De Lotto³⁰, L. Del Peral⁴¹, R. de Menezes³⁴, G. De Palma²², C. Díaz²¹, A. Di Piano²⁷, F. Di Pierro³⁴, R. Di Triá³³, L. Di Venere⁴², D. Dominis Prester⁴³, A. Donini¹⁰, D. Dörner⁴⁴, M. Doro¹², L. Eisenberger⁴⁴, D. Elsässer⁴⁵, G. Emery²⁶, L. Feligioni²⁶, F. Ferrarotto⁴⁶, A. Fiasson^{14,47}, L. Foffano³², F. Frías García-Lago¹³, S. Fröse⁴⁵, Y. Fukazawa⁴⁸, S. Gallozzi¹⁰, R. García López¹³, S. García Soto²¹, C. Gasbarra⁴⁹, D. Gasparrini⁴⁹, J. Giesbrecht Paiva²⁰, N. Giglietto²², F. Giordano³³, N. Godinovic⁵⁰, T. Gradetzke⁴⁵, R. Grau²³, L. Greaux¹⁹, D. Green¹¹, J. Green¹¹, S. Gunji⁵¹, P. Günther⁴⁴, J. Hackfeld¹⁹, D. Hadash², A. Hahn¹¹, M. Hashizume⁴⁸, T. Hassan²¹, K. Hayashi^{52,2}, L. Heckmann^{11,53}, M. Heller³¹, J. Herrera Llorente¹³, K. Hirotani², D. Hoffmann²⁶, D. Horns¹⁵, J. Houles³⁶, M. Hrabovsky³⁶, D. Hrupec⁵⁴, D. Hui^{55,2}, M. Iarlori⁵⁶, R. Imazawa⁴⁸, T. Inada², Y. Inome², S. Inoue^{57,2}, K. Ioka⁵⁸, M. Iori⁴⁶, T. Itokawa², A. Iuliano⁹, J. Jahanvi³⁰, I. Jimenez Martinez¹¹, J. Jimenez Quiles²³, I. Jorge Rodrigo²¹, J. Jurysck⁵⁹, M. Kagaya^{52,2}, O. Kalashev⁶⁰, V. Karas⁶¹, H. Katagiri⁶², D. Kerszberg^{23,63}, M. Kherlakian¹⁹, T. Kiyomoto⁶⁴, Y. Kobayashi², K. Kohri⁶⁵, A. Kong², P. Kornecki¹, H. Kubo², J. Kushida¹, B. Lacave³¹, M. Lainé¹⁷, G. Lamanna¹⁴, A. Lamastra¹⁰, L. Lemoigne¹⁴, M. Linhof⁴⁵, S. Lombardi¹⁰, F. Longo⁶⁶, R. López-Coto⁷, M. López-Moya¹⁷, A. López-Oramas¹³, S. Loporchio³³, A. Lorini³, J. Lozano Bahilo⁴¹, F. Lucarelli¹⁰, H. Luciani⁶⁶, P. L. Luque-Escamilla⁶⁷, P. Majumdar^{68,2}, M. Makariev⁶⁹, M. Mallamaci^{37,38}, D. Mandat⁵⁹, M. Manganaro⁴³, D. K. Maniadas¹⁰, G. Manicò³⁸, K. Mannheim⁴⁴, S. Marchesi^{28,27,70}, F. Marini¹², M. Mariotti¹², P. Marquez⁷¹, G. Marsella^{38,37}, J. Martí⁶⁷, O. Martinez^{72,73}, G. Martínez²¹, M. Martínez²³, A. Mas-Aguilar¹⁷, M. Massa³, G. Maurin¹⁴, D. Mazin^{2,11}, J. Méndez-Gallego⁷, S. Menon^{10,74}, E. Mestre Guillén¹⁵, D. Miceli¹², T. Miener¹⁷, J. M. Miranda⁷², R. Mirzoyan¹¹, M. Mizote⁷⁶, T. Mizuno⁴⁸, M. Molero Gonzalez¹³, E. Molina¹³, T. Montaruli³¹, A. Moralejo²³, D. Morcuende⁷, A. Moreno Ramos⁷², A. Morselli⁴⁹, V. Moya¹⁷, H. Muraishi⁷⁷, S. Nagataki⁷⁸, T. Nakamori⁵¹, C. Nanci²⁷, A. Neronov⁶⁰, D. Nieto Castañó¹⁷, M. Nieves Rosillo¹³, L. Nikolic³, K. Nishijima¹, K. Noda^{57,2}, D. Nosek⁷⁹, V. Novotny⁷⁹, S. Nozaki², M. Ohishi², Y. Ohtani², T. Oka⁸⁰, A. Okumura^{81,82}, R. Orto⁸³, L. Orsini³, J. Otero-Santos⁷, P. Ottanelli⁸⁴, M. Palatiello¹⁰, G. Panebianco²⁷, D. Paneque¹¹, F. R. Pantaleo²², R. Paoletti³, M. Paredes⁶, M. Pech^{59,36}, M. Pecimotika²³, M. Peresano¹¹, F. Pfeifle⁴⁴, E. Pietropaolo⁵⁶, M. Pihet⁶, G. Pirola¹¹, C. Plard¹⁴, F. Podobnik³, M. Polo²¹, E. Prandini¹², M. Prouza⁵⁹, S. Rainò³³, R. Rando¹², W. Rhode⁴⁵, M. Ribó⁶, V. Rizzi⁵⁶, G. Rodríguez Fernandez⁴⁹, M. D. Rodríguez Frías⁴¹, P. Romano²⁴, A. Roy⁴⁸, A. Ruina¹², E. Ruiz-Velasco¹⁴, T. Saitō², S. Sakurai², D. A. Sanchez¹⁴, H. Sano^{85,2}, T. Šarić⁵⁰, Y. Sato⁸⁶, F. G. Saturni¹⁰, V. Savchenko⁶⁰, F. Schiavone³³, B. Schleicher⁴⁴, F. Schmuckermayer¹¹, F. Schussler³⁹, T. Schweizer¹¹, M. Seglar Arroyo²³, T. Sieger⁴⁴, G. Silvestri⁴³, A. Simongini^{10,74}, J. Sitarek²⁵, V. Sliusar⁸, I. Sofia³⁴, A. Stamerra¹⁰, J. Striško⁵⁴, M. Strzys², Y. Suda⁴⁸, A. Sunny^{10,74}, H. Tajima⁸¹, M. Takahashi⁸¹, J. Takata², R. Takeishi², P. H. T. Tam², S. J. Tanaka⁸⁶, D. Tateishi⁶⁹, T. Tavernier⁵⁹, P. Temnikov⁶⁹, Y. Terada⁶⁴, K. Terauchi⁸⁰, M. Teshima^{11,2}, M. Tluczykont¹⁵, F. Tokana⁵¹, T. Tomura², D. F. Torres⁷⁵, F. Tramonti³, P. Travnicek⁵⁹, G. Tripodo³⁸, A. Tutone¹⁰, M. Vacula³⁶, J. van Scherpenberg¹¹, M. Vázquez Acosta¹³, S. Ventura³, S. Vercellone²⁴, G. Verna³, I. Viale¹², A. Vighiano³⁰, C. F. Vignorito^{34,35}, E. Visentin^{34,35}, V. Vitale⁴⁹, V. Voisekhovsky³¹, G. Voutsinas³¹, I. Vovk², T. Vuillaume¹⁴, R. Walter⁵, L. Wan², J. Wójciewicz²⁵, T. Yamamoto⁷⁶, R. Yamazaki⁸⁶, Y. Yao¹, P. K. H. Yeung², T. Yoshida⁶², T. Yoshikoshi², W. Zhang⁷⁵, The CTAO-LST Project

¹Department of Physics, Tokai University, 4-1-1, Kita-Kaname, Hiratsuka, Kanagawa 259-1292, Japan. ²Institute for Cosmic Ray Research, University of Tokyo, 5-1-5, Kashiwa-no-ha, Kashiwa, Chiba 277-8582, Japan. ³INFN and Università degli Studi di Siena, Dipartimento di Scienze Fisiche, della Terra e dell'Ambiente (DSFTA), Sezione di Fisica, Via Roma 56, 53100 Siena, Italy. ⁴Université Paris-Saclay, Université Paris Cité, CEA, CNRS, AIM, F-91191 Gif-sur-Yvette Cedex, France. ⁵FLSALC IRL 2009, CNRS/IAC, La Laguna, Tenerife, Spain. ⁶Departament de Física Quàntica i Astrofísica, Institut de Ciències del Cosmos, Universitat de Barcelona, IECC-UB, Martí i Franquès, 1, 08028, Barcelona, Spain. ⁷Instituto de Astrofísica de Andalucía-CSIC, Glorieta de la Astronomía s/n, 18008, Granada, Spain. ⁸Department of Astronomy, University of Geneva, Chemin d'Ecogia 16, CH-1290 Versoix, Switzerland. ⁹INFN Sezione di Napoli, Via Cintia, ed. G, 80126 Napoli, Italy. ¹⁰INAF - Osservatorio Astronomico di Roma, Via di Frascati 33, 00040, Monteporzio Catone, Italy. ¹¹Max-Planck-Institut für Physik, Boltzmannstraße 8, 85748 Garching bei München. ¹²INFN Sezione di Padova and Università degli Studi di Padova, Via Marzolo 8, 35131 Padova, Italy. ¹³Instituto de Astrofísica de Canarias and Departamento de Astrofísica, Universidad de La Laguna, C. Via Láctea, s/n, 38205 La Laguna, Santa Cruz de Tenerife, Spain. ¹⁴Univ. Savoie Mont Blanc, CNRS, Laboratoire d'Annecy de Physique des Particules - IN2P3, 74000 Annecy, France. ¹⁵Universität Hamburg, Institut für Experimentalphysik, Luruper Chaussee 149, 22761 Hamburg, Germany. ¹⁶Graduate School of Science, University of Tokyo, 7-3-1 Hongo, Bunkyo-ku, Tokyo 113-0033, Japan. ¹⁷IPARCOS-UCM, Instituto de Física de Partículas y del Cosmos, and EMFTEL Department, Universidad Complutense de Madrid, Plaza de Ciencias, 1. Ciudad Universitaria, 28040 Madrid, Spain. ¹⁸Faculty of Science and Technology, Universidad del Azuay, Cuenca, Ecuador. ¹⁹Institut für Theoretische Physik, Lehrstuhl IV: Plasma-Astroteilchenphysik, Ruhr-Universität Bochum, Universitätsstraße 150, 44801 Bochum, Germany. ²⁰Centro Brasileiro de Pesquisas Físicas, Rua Xavier Sigaud 150, RJ 22290-180, Rio de Janeiro, Brazil. ²¹CIEMAT, Avda. Complutense 40, 28040 Madrid, Spain. ²²INFN Sezione di Bari and Politecnico di Bari, via Orabona 4, 70124 Bari, Italy. ²³Instituto de Física d'Altes Energies (IFAE), The Barcelona Institute of Science and Technology, Campus UAB, 08193 Bellaterra (Barcelona), Spain. ²⁴INAF - Osservatorio Astronomico di Brera, Via Brera 28, 20121 Milano, Italy. ²⁵Faculty of Physics and Applied Informatics, University of Lodz, ul. Pomorska 149-153, 90-236 Lodz, Poland. ²⁶Aix Marseille Univ, CNRS/IN2P3, CPPM, Marseille, France. ²⁷INAF - Osservatorio di Astrofisica e Scienza dello spazio di Bologna, Via Piero Gobetti 93/3, 40129 Bologna, Italy. ²⁸Dipartimento di Fisica e Astronomia (DIFA) Augusto Righi, Università di Bologna, via Gobetti 93/2, I-40129 Bologna, Italy. ²⁹Lamarr Institute for Machine Learning and Artificial Intelligence, 44227 Dortmund, Germany. ³⁰INFN Sezione di Trieste and Università degli studi di Udine, via delle scienze 206, 33100 Udine, Italy. ³¹University of Geneva - Département de physique nucléaire et corpusculaire, 24 Quai Ernest Ansermet, 1211 Genève 4, Switzerland. ³²INAF - Istituto di Astrofisica e Planetologia Spaziali (IAPS), Via del Fosso del Cavaliere 100, 00133 Roma, Italy. ³³INFN Sezione di Bari and Università di Bari, via Orabona 4, 70126 Bari, Italy. ³⁴INFN Sezione di Torino, Via P. Giuria 1, 10125 Torino, Italy. ³⁵Dipartimento di Fisica - Università degli Studi di Torino, Via Pietro Giuria 1 - 10125 Torino, Italy. ³⁶Palacky University Olomouc, Faculty of Science, 17. listopadu 1192/12, 771 46 Olomouc, Czech Republic. ³⁷Dipartimento di Fisica e Chimica 'E. Segre' Università degli Studi di Palermo, via delle Scienze, 90128 Palermo. ³⁸INFN Sezione di Catania, Via S. Sofia 64, 95123 Catania, Italy. ³⁹IRFU, CEA, Université Paris-Saclay, Bât 141, 91191 Gif-sur-Yvette, France. ⁴⁰Port d'Informació Científica, Edifici D, Carrer de l'Albareda, 08193 Bellaterra (Cerdanyola del Vallès), Spain. ⁴¹University of Alcalá UAH, Departamento de Physics and Mathematics, Pza. San Diego, 28801, Alcalá de Henares, Madrid, Spain. ⁴²INFN Sezione di Bari, via Orabona 4, 70125, Bari, Italy. ⁴³University of Rijeka, Department of Physics, Radmile Matejčić 2, 51000 Rijeka, Croatia. ⁴⁴Institute for Theoretical Physics and Astrophysics, Universität Würzburg, Campus Hubland Nord, Emil-Fischer-Str. 31, 97074 Würzburg, Germany. ⁴⁵Department of Physics, TU Dortmund University, Otto-Hahn-Str. 4, 44227 Dortmund, Germany. ⁴⁶INFN Sezione di Roma La Sapienza, P.le Aldo Moro, 2 - 00185 Rome, Italy. ⁴⁷ILANCE, CNRS - University of Tokyo International Research Laboratory, University of Tokyo, 5-1-5 Kashiwa-no-Ha Kashiwa City, Chiba 277-8582, Japan. ⁴⁸Physics Program, Graduate School of Advanced Science and Engineering, Hiroshima University, 1-3-1 Kagamiyama, Higashi-Hiroshima City, Hiroshima, 739-8526, Japan. ⁴⁹INFN Sezione di Roma Tor Vergata, Via della Ricerca Scientifica 1, 00133 Rome, Italy. ⁵⁰University of Split, FESB, R. Boškovića 32, 21000 Split, Croatia. ⁵¹Department of Physics, Yamagata University, 1-4-12 Kojirakawa-machi, Yamagata-shi, 990-8560, Japan. ⁵²Sendai College, National Institute of Technology, 4-16-1 Ayashi-Chuo, Aoba-ku, Sendai city, Miyagi 989-3128, Japan. ⁵³Université Paris Cité, CNRS, Astroparticule et Cosmologie, F-75013 Paris, France. ⁵⁴Josip Juraj Strossmayer University of Osijek, Department of Physics, Trg Ljudevita Gaja 6, 31000 Osijek, Croatia. ⁵⁵Department of Astronomy and Space Science, Chungnam National University, Daejeon 34134, Republic of Korea. ⁵⁶INFN Dipartimento di Scienze Fisiche e Chimiche - Università degli Studi dell'Aquila and Gran Sasso Science Institute, Via Vetoio 1, Viale Crispi 7, 67100 L'Aquila, Italy. ⁵⁷Chiba University, 1-33, Yayoi-cho, Inage-ku, Chiba-shi, Chiba, 263-8522 Japan. ⁵⁸Kitashirakawa Oiwa-kecho, Sakyo Ward, Kyoto, 606-8502, Japan. ⁵⁹FZU - Institute of Physics of the Czech Academy of Sciences, Na Slovance 1999/2, 182 21 Praha 8, Czech Republic. ⁶⁰Laboratory for High Energy Physics, Ecole Polytechnique Fédérale, CH-1015 Lausanne, Switzerland. ⁶¹Astronomical Institute of the Czech Academy of Sciences, Bocni II 1401 - 14100 Prague, Czech Republic. ⁶²Faculty of Science, Ibaraki University, 2 Chome-1-1 Bunkyo, Mito, Ibaraki 310-0056, Japan. ⁶³Sorbonne Université, CNRS/IN2P3, Laboratoire de Physique Nucléaire et de Hautes Energies, LPNHE, 4 place Jussieu, 75005 Paris, France. ⁶⁴Graduate School of Science and Engineering, Saitama University, 255 Simo-Ohkubo, Sakura-ku, Saitama city, Saitama 338-8570, Japan. ⁶⁵Institute of Particle and Nuclear Studies, KEK (High Energy Accelerator Research Organization), 1-1 Oho, Tsukuba, 305-0801, Japan. ⁶⁶INFN Sezione di Trieste and Università degli Studi di Trieste, Via Valerio 2, 34127 Trieste, Italy. ⁶⁷Escuela Politécnica Superior de Jaén, Universidad de Jaén, Campus Las Lagunillas s/n, Edif. A3, 23071 Jaén, Spain. ⁶⁸Saha Institute of Nuclear Physics, A CI of Homi Bhabha National Institute, Kolkata 700064, West Bengal, India. ⁶⁹Institute for Nuclear Research and Nuclear Energy, Bulgarian Academy of Sciences, 72 boul. Tsigradgradsko chaussee, 1784 Sofia, Bulgaria. ⁷⁰Department of Physics and Astronomy, Clemson University, Kinard Lab of Physics, Clemson, SC 29634, USA. ⁷¹Institut de Física d'Altes Energies (IFAE), The Barcelona Institute of Science and Technology, Campus UAB, 08193 Bellaterra (Barcelona), Spain. ⁷²Grupo de Electronica, Universidad Complutense de Madrid, Av. Complutense s/n, 28040 Madrid, Spain. ⁷³E.S.C.C. Experimentales y Tecnología (Departamento de Biología y Geología, Física y Química Inorgánica) - Universidad Rey Juan Carlos. ⁷⁴Macroarea di Scienze MMFFNN, Università di Roma Tor Vergata, Via della Ricerca Scientifica 1, 00133 Rome, Italy. ⁷⁵Institute of Space Sciences (ICE, CSIC), and Institut d'Estudis Espacials de Catalunya (IEEC), and Institució Catalana de Recerca i Estudis Avançats (ICREA), Campus UAB, Carrer de Can Magrans, s/n 08193 Bellaterra, Spain. ⁷⁶Department of Physics, Konan University, 8-9-1 Okamoto, Higashinada-ku Kobe 658-8501, Japan. ⁷⁷School of Allied Health Sciences, Kitasato University, Sagamihara, Kanagawa 228-8555, Japan. ⁷⁸RIKEN, Institute of Physical and Chemical Research, 2-1 Hirosawa, Wako, Saitama, 351-0198, Japan. ⁷⁹Charles University, Institute of Particle

and Nuclear Physics, V Holešovičkách 2, 180 00 Prague 8, Czech Republic. ⁸⁰Division of Physics and Astronomy, Graduate School of Science, Kyoto University, Sakyo-ku, Kyoto, 606-8502, Japan. ⁸¹Institute for Space-Earth Environmental Research, Nagoya University, Chikusa-ku, Nagoya 464-8601, Japan. ⁸²Kobayashi-Maskawa Institute (KMI) for the Origin of Particles and the Universe, Nagoya University, Chikusa-ku, Nagoya 464-8602, Japan. ⁸³Graduate School of Technology, Industrial and Social Sciences, Tokushima University, 2-1 Minamijosanjima, Tokushima, 770-8506, Japan. ⁸⁴INFN Sezione di Pisa, Edificio C – Polo Fibonacci, Largo Bruno Pontecorvo 3, 56127 Pisa, Italy. ⁸⁵Gifu University, Faculty of Engineering, 1-1 Yanagido, Gifu 501-1193, Japan. ⁸⁶Department of Physical Sciences, Aoyama Gakuin University, Fuchinobe, Sagami-hara, Kanagawa, 252-5258, Japan.

Acknowledgments

We gratefully acknowledge financial support from the following agencies and organisations: Conselho Nacional de Desenvolvimento Científico e Tecnológico (CNPq), Fundação de Amparo à Pesquisa do Estado do Rio de Janeiro (FAPERJ), Fundação de Amparo à Pesquisa do Estado de São Paulo (FAPESP), Fundação de Apoio à Ciência, Tecnologia e Inovação do Paraná - Fundação Araucária, Ministry of Science, Technology, Innovations and Communications (MCTIC), Brasil; Ministry of Education and Science, National RI Roadmap Project DO1-153/28.08.2018, Bulgaria; Croatian Science Foundation (HrZZ) Project IP-2022-10-4595, Rudjer Boskovic Institute, University of Osijek, University of Rijeka, University of Split, Faculty of Electrical Engineering, Mechanical Engineering and Naval Architecture, University of Zagreb, Faculty of Electrical Engineering and Computing, Croatia; Ministry of Education, Youth and Sports, MEYS LM2023047, EU/MEYS CZ.02.1.01/0.0/0.0/16_013/0001403, CZ.02.1.01/0.0/0.0/18_046/0016007, CZ.02.1.01/0.0/0.0/16_019/0000754, CZ.02.01.01/00/22_008/0004632 and CZ.02.01.01/00/23_015/0008197 Czech Republic; CNRS-IN2P3, the French Programme d'investissements d'avenir and the Enigmass Labex, This work has been done thanks to the facilities offered by the Univ. Savoie Mont Blanc - CNRS/IN2P3 MUST computing center, France; Max Planck Society, German Bundesministerium für Bildung und Forschung (Verbundforschung / ErUM), Deutsche Forschungsgemeinschaft (SFBs 876 and 1491), Germany; Istituto Nazionale di Astrofisica (INAF), Istituto Nazionale di Fisica Nucleare (INFN), Italian Ministry for University and Research (MUR), and the financial support from the European Union – Next Generation EU under the project IR0000012 - CTA+ (CUP C53C22000430006), announcement N.3264 on 28/12/2021: "Rafforzamento e creazione di IR nell'ambito del Piano Nazionale di Ripresa e Resilienza (PNRR)"; ICRR, University of Tokyo, JSPS, MEXT, Japan; JST SPRING - JP-MJSP2108; Narodowe Centrum Nauki, grant number 2023/50/A/ST9/00254, Poland; The Spanish groups acknowledge the Spanish Ministry of Science and Innovation and the Spanish Research State Agency (AEI) through the government budget lines PGE2022/28.06.000X.711.04, 28.06.000X.411.01 and 28.06.000X.711.04 of PGE 2023, 2024 and 2025, and grants PID2019-104114RB-C31, PID2019-107847RB-C44, PID2019-104114RB-C32, PID2019-105510GB-C31, PID2019-104114RB-C33, PID2019-107847RB-C43, PID2019-107847RB-C42, PID2019-107988GB-C22, PID2021-124581OB-I00, PID2021-125331NB-I00, PID2022-136828NB-C41, PID2022-137810NB-C22, PID2022-138172NB-C41, PID2022-138172NB-C42, PID2022-138172NB-C43, PID2022-139117NB-C41, PID2022-139117NB-C42, PID2022-139117NB-C43, PID2022-139117NB-C44, PID2022-136828NB-C42, PDC2023-145839-I00 funded by the Spanish MCIN/AEI/10.13039/501100011033 and "and by ERDF/EU and NextGenerationEU PRTR; the "Centro de Excelencia Severo Ochoa" program through grants no. CEX2019-000920-S, CEX2020-001007-S, CEX2021-001131-S; the "Unidad de Excelencia María de Maeztu" program through grants no. CEX2019-000918-M, CEX2020-001058-M; the "Ramón y Cajal" program through grants RYC2021-032991-I funded by MICIN/AEI/10.13039/501100011033 and the European Union "NextGenerationEU"/PRTR and RYC2020-028639-I; the "Juan de la Cierva-Incorporación" program through grant no. IJC2019-040315-I and "Juan de la Cierva-formación" through grant JDC2022-049705-I. They also acknowledge the "Atracción de Talento" program of Comunidad de Madrid through grant no. 2019-T2/TIC-12900; the project "Tecnologías avanzadas para la exploración del universo y sus componentes" (PR47/21 TAU), funded by Comunidad de Madrid, by the Recovery, Transformation and Resilience Plan from the Spanish State, and by NextGenerationEU from the European Union through the Recovery and Resilience Facility; "MAD4SPACE: Desarrollo de tecnologías habilitadoras para estudios del espacio en la Comunidad de Madrid" (TEC-2024/TEC-182) project funded by Comunidad de Madrid; the La Caixa Banking Foundation, grant no. LCF/BQ/PI21/11830030; Junta de Andalucía under Plan Complementario de I+D+I (Ref. AST22_0001) and Plan Andaluz de Investigación, Desarrollo e Innovación as research group FQM-322; Project ref. AST22_00001_9 with funding from NextGenerationEU funds; the "Ministerio de Ciencia, Innovación y Universidades" and its "Plan de Recuperación, Transformación y Resiliencia"; "Consejería de Universidad, Investigación e Innovación" of the regional government of Andalucía and "Consejo Superior de Investigaciones Científicas", Grant CNS2023-144504 funded by MICIU/AEI/10.13039/501100011033 and by the European Union NextGenerationEU/PRTR, the European Union's Recovery and Resilience Facility-Next Generation, in the framework of the General Invitation of the Spanish Government's public business entity Red.es to participate in talent attraction and retention programmes within Investment 4 of Component 19 of the Recovery, Transformation and Resilience Plan; Junta de Andalucía under Plan Complementario de I+D+I (Ref. AST22_00001), Plan Andaluz de Investigación, Desarrollo e Innovación (Ref. FQM-322). "Programa Operativo de Crecimiento Inteligente" FEDER 2014-2020 (Ref. ESFRI-2017-IAC-12), Ministerio de Ciencia e Innovación, 15% co-financed by Consejería de Economía, Industria, Comercio y Conocimiento del Gobierno de Canarias; the "CERCA" program and the grants 2021SGR00426 and 2021SGR00679, all funded by the Generalitat de Catalunya; and the European Union's NextGenerationEU (PRTR-C17.11). This research used the computing and storage resources provided by the Port d'Informació Científica (PIC) data center. State Secretariat for Education, Research and Innovation (SERI) and Swiss National Science Foundation (SNSF), Switzerland; The research leading to these results has received funding from the European Union's Seventh Framework Programme (FP7/2007-2013) under grant agreements No 262053 and No 317446; This project is receiving funding from the European Union's Horizon 2020 research and innovation programs under agreement No 676134; ESCAPE - The European Science Cluster of Astronomy & Particle Physics ESFRI Research Infrastructures has received funding from the European Union's Horizon 2020 research and innovation programme under Grant Agreement no. 824064.